Journal of Materials and Environmental Science
ISSN : 2028-2508
e-ISSN : 2737-890X
CODEN : JMESCN

J. Mater. Environ. Sci., 2025, Volume 16, Issue 5, Page 798-813

http://www.jmaterenvironsci.com

Analysis and modeling of the erosive power of rainfall events measured in Northern Benin

Loïc Saturnin ADJIKPE[1*], Hilaire KOUGBEAGBEDE[1], François K. GUEDJE[1], Sounmaïla MOUMOUNI[2] et Massou Siaka[1]**

[1]Faculté des Sciences et Techniques, Université d'Abomey-Calavi, Bénin
[2]Ecole Normale Supérieure de Natitingou, Université Nationale des Sciences, Technologies, Ingénierie et Mathématiques (UNSTIM), Natitingou, Bénin

**Corresponding Author; Email Address: adjikpel@gmail.com*
***Corresponding Author; Email Address: hilars83@gmail.com*

Received *09 Oct 2024,*
Revised *20 Apr 2025,*
Accepted *21 Apr 2025*

Keywords:
- ✓ *Erosive power;*
- ✓ *Rainfall event;*
- ✓ *Erosivity factor;*
- ✓ *Kinetic energy;*
- ✓ *Rainfall intensity.*

Citation*: Adjikpé L.S., Kougbéagbédé H., Guédjé K.F., Moumouni S. et Massou S. (2025). Analysis and modeling of the erosive power of rainfall events measured in Northern Benin, J. Mater. Environ. Sci., 16(5), 798-813*

Abstract: This study proposes an approach for analyzing and modeling the erosive power of rainfall events to predict and assess the erosive risk based on the drop size distribution (DSD) of rain. The analysis relied on the proportions of identified potentially erosive rainfall events, cumulative rainfall amounts, and total kinetic energy. The modeling involved establishing two models R_j-KE_j and R_j-I_j to estimate the erosivity factor R_j from the total kinetic energy KE_j and the intensity I_j of a potentially erosive rainfall event j, respectively. Statistical criteria were used to evaluate the ability of these models to estimate the erosivity factor of any erosive rainfall event. The analysis revealed that 40.86% of all rainfall events are potentially erosive, with peaks in cumulative amounts and kinetic energy. The study further revealed that 71.29% of the total cumulative rainfall and 76.65% of the total kinetic energy come from these erosive rainfall events, which are responsible for the majority of the erosive risk associated with precipitation. The statistical criteria values demonstrated the effectiveness of the two models R_j-KE_j and R_j-I_j in reproducing the erosivity factor of any erosive rainfall event.

1. Introduction

Understanding the erosive power of precipitation is fundamental in any strategy to combat water erosion caused by rain. This knowledge is crucial as it helps predict erosive risk due to rainfall, in order to take the necessary precautions to prevent related damage such as sedimentation of dams, soil surface stripping, damage to road infrastructure, etc. The erosive power of a rainfall event depends on the characteristics of the raindrops (size, speed, shape, and impact angle), the rainfall event itself (type, intensity, and duration), and is evaluated using an indicator known as the erosivity factor (or index) of rain. This factor characterizes the erosive force of precipitation on soil. Its calculation requires instantaneous rainfall measurements (pluviograms), which are not always available over long periods (Renard et al., 1994). To circumvent this difficulty, Wischmeier and Smith (1978), pioneers in this study, determined the rain erosivity factor based on total kinetic energy and maximum rainfall intensity over thirty minutes in the absence of data on raindrop distribution. Most subsequent studies worldwide have determined the erosivity index from daily (Richardson et al., 1983; Petkovsek and Mikos, 2004), monthly (Grimm et al., 2003), annual (Renard and Freimund, 1994; Brown and Foster, 1987; etc.), and interannual (Arnoldus, 1977) rainfall data.

Surprised by the number of papers collected from Scopus using "rainfall & modelling" higher than 43,500 documents. This finding reflects the importance of deciders makers to supervise the phenomenon to limit damages. A bibliometric analysis should be necessary to visualize the most published authors, concerned countries… (Cuéllar-Rojas et al., 2022; N'diaye et al., 2022; Alsadi et al., 2024; Hammouti et al., 2025). The analysis was limited from 2018 to 2024 to get <20,000 documents to apply VOS viewer mapping. **Figure 1** indicates the increase of articles with time to reach over 3000 articles in 2024. All parts of the world are concerned by the rainfall last time due to climate changes. China, the US, India, Australia, Iran, Brazil, France are mentioned by large nodes to indicate the preoccupation by the rainfall (**Figure 2**) and quantitively presented in **Figure 3**. In this studied period, some researchers are distinguished by their production to see Prof Shahid from Malaysia (>42 papers) and has a total of 462 articles, H=75 and about 18,000 citations (**Figure 4**). But, during all years, Singh V.P. is the most published one (>1680 articles, H=111 and 62,700 citations). His article on drought concepts is the most published paper (>3900 times) (Mishra & Singh, (2010).

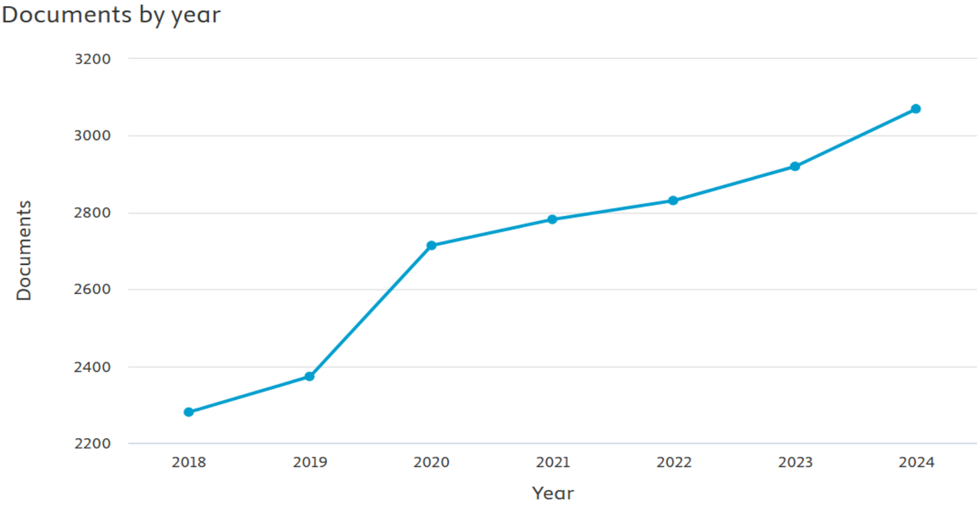

Figure 1. Evolution of articles per year

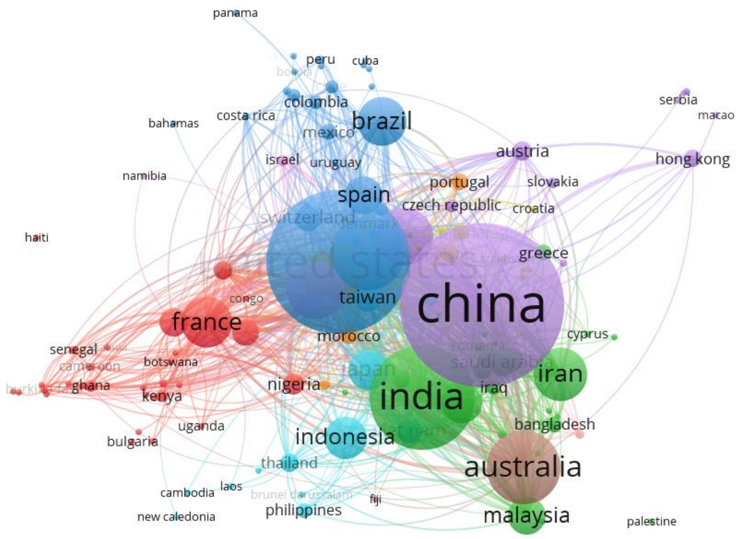

Figure 2. Countries preoccupied by the rainfall

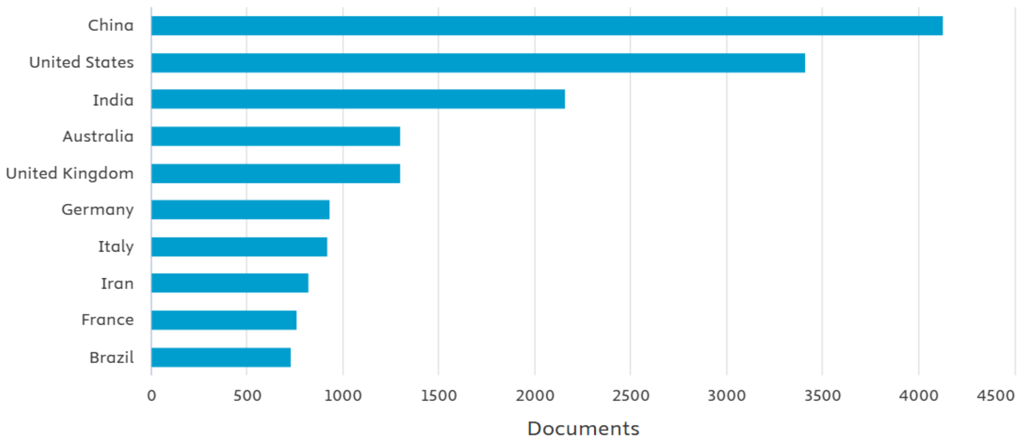

Figure 3 Quantitative measure of the most countries suffering from the rainfall

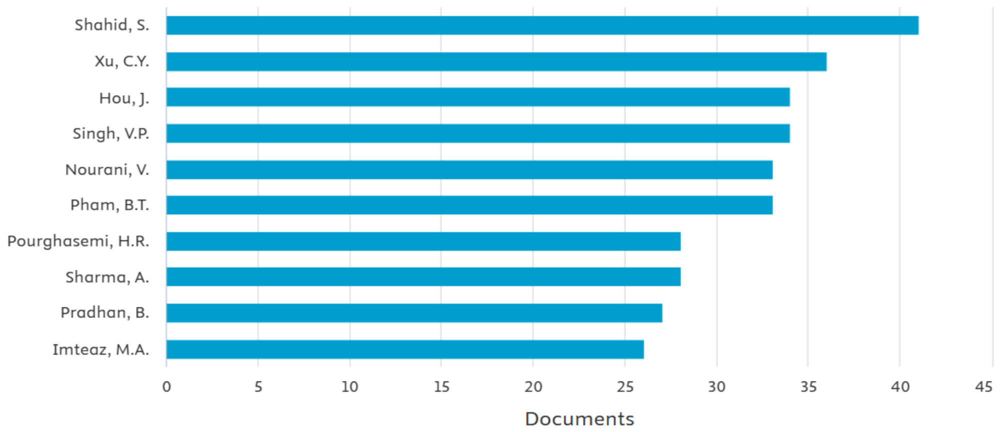

Figure 4 Prolife Authors

The mapping obtained using VOS viewer confirms the importance of this field by the presence of numerous of nodes at different colors forming clusters showing the collaboration between researchers and institutions and their countries (Salim et al., 2022; Lrhoul et al., 2023; Mehta N., Kozielska, 2024).

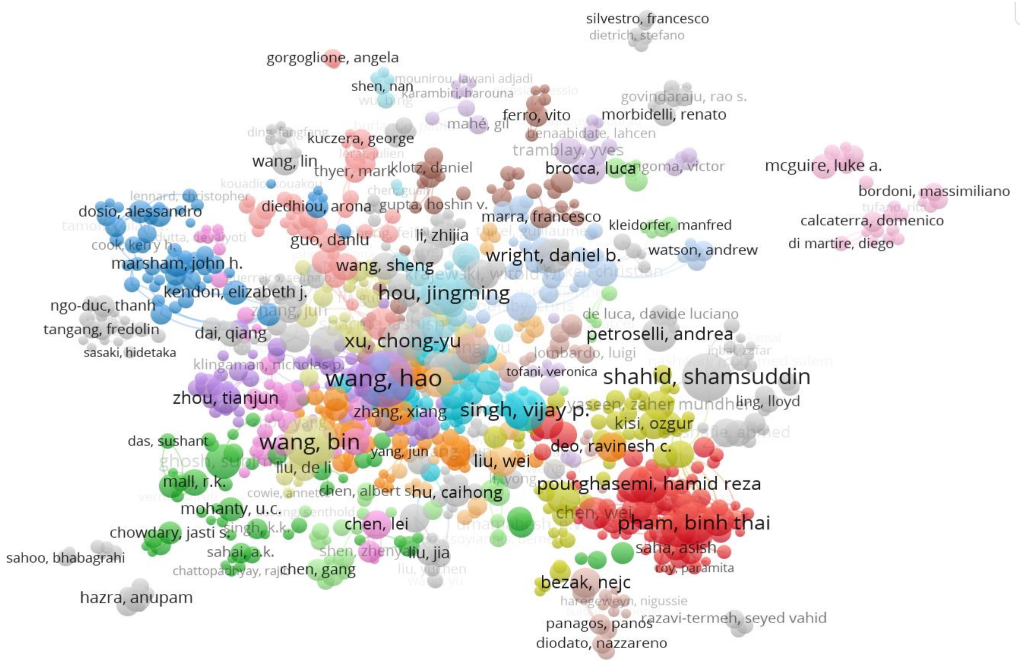

Figure 5. Author's mapping and coworking on VOS viewer

In Benin, since the availability of DSD data measured in Northwest Benin from 2005 to 2007, no study has focused on analyzing and modeling the erosive power of a rainfall event using these DSD data. A recent study by ADJIKPE et al. (2021) based on these DSD data only established estimators of the kinetic energy of raindrops from measurable hydrological variables: rainfall intensity and radar reflectivity factor under Rayleigh conditions. The purpose of the present study is to: (i) analyze the erosive power of precipitation and identify types of rainfall events responsible for erosive risk; (ii) develop two models R_j-KE_j and R_j-I_j to estimate the erosivity factor R_j from total kinetic energy KE_j and the intensity I_j of a potentially erosive rainfall event j. This article is organized as follows: after the introduction, the first part describes the study area and the data used; the second part is dedicated to the methodology used, and the third part presents the results followed by discussions.

2. Methodology

2.1-Experiments

Three optical disdrometers single-beam and dual-beam (Salle et al., 1998; Löffler-Mang and Joss ,2000; Delahaye et al., 2005) were installed at three sites chosen in the northwest of Benin, specifically in Nangatchiori, Djougou, and Copargo, from 2005 to 2007 (Moumouni et al., 2008). These sensors sampled 1-minute DSD spectra. A dataset composed of 11.647 DSD spectra of rain intensities greater than or equal to 0.1 mm•h^{-1} divided into 93 rain events of duration at least equal to 15 min with an intermittency of less than 30 min (Moumouni et al., 2023) is thus constituted. These DSD data have been extensively validated by several studies [Gosset et al. (2010), Kougbéagbédé et al. (2017), Moumouni et al. (2008, 2018, 2021, 2023), and ADJIKPE et al. (2021)]. These rainfall events are either erosive or non-erosive. According to Wischmeier and Smith (1978), a rainfall event is considered erosive if the corresponding rainfall height is greater than 12.7 mm and the minimum inter-event time (MIT) is greater than 6 h, except for rainfall events whose height reaches 6.35 mm in 15 min. Several years later, the work of Dunkerley (2008, 2010) qualified this threshold as arbitrary, given that the number and properties of rainfall events (mean duration, height, mean rainfall rate, mean inter-event time, intra-event variability, rainfall peak, etc.) change both in time and space with the selected MIT.

In this study, we considered potentially erosive rainfall events to be events lasting at least 15 min with an intermittency of less than 30 min and whose cumulative height of precipitated water is greater than 12.7 min. This height threshold is chosen for the same reasons as Wischméier and Smith (1978). Thus, out of the 93 rainfall events, 38 were identified as potentially erosive and constitute the DATA X sample. If these rainfall events are of long duration, the presence of gaps between the spectra can significantly modify the average rainfall intensity (Huff, 1967). This is why, for the reliability and relevance of the calculation of the values of the average rainfall intensities, we extracted from the DATA X sample those whose spectra are recorded with the fewest possible gaps (i.e. the duration in minutes of the rainfall event corresponds to the number of 1-minute spectra recorded to within a few minutes). A new sample composed of 17 erosive rainfall events with quasi-continuous recording of rain DSD spectra called DATA Y is then created and used for modeling.

2.2 - Analysis of the Erosive Power of Rain

To analyze the erosive power of the rainfall events in our dataset, we first identified the erosive rainfall events by site according to the criteria described in section 1.2.2. Secondly, we evaluated the contribution of these erosive rainfall events to the aggressiveness of the rain in our study area.

Furthermore, hydrological variables, specifically maximum intensity (I_{max}), event total (Het), and the total kinetic energy of the potentially erosive rainfall events were analyzed and compared to those of all rainfall events. Thus, the rainfall events responsible for the soil erosion risk are identified.

2.3- Modeling the Erosivity Factor of an Erosive Rainfall Event

Since the pioneering work of Wischmeier and Smith (1978), who calculated the erosivity factor of rain in the absence of data on the diameter and fall velocity of raindrops using the following formula (1):

$$R_j = aKE_j \cdot (I_{30,max})_j \quad (1)$$

où R_j, $(I_{30,max})_j$ et $(KE)_j$ $R_j = aKE_j \cdot (I_{30,max})_j$ represent the erosivity factor, the maximum intensity over 30 minutes, and the total kinetic energy of a rainfall event (j); (a) is a multiplication factor related to the chosen unit system (where (a = 1/87.6) when R_j is expressed in MJ.mm.ha^{-1}.an^{-1}.h^{-1}). However, the lack of data on the parameters (KE_j and $I_{30,max}$ has led some researchers to establish relationships between kinetic energy (KE) and rainfall intensity (I) and simple models relating the erosivity factor to rainfall amount over different time intervals (daily, monthly, annually) (see **Table 1 and Table 2**).

Table 1: Some KE-I models developed in various studies:

Reference	Form of model	Equation	Location
Steiner and Smith (2000) ADJIKPE et al. (2021) Jan Pétru (2018) Nan Yu (2012)	Power law	$KE = aI^b$	Mississippi (USA) Northen of Benin Czech Republic South of France
McGregor et al. (1995) Brown and Foster (1987)	Exponential model	$KE = a[1-b\exp(-\lambda I)$	Hong Kong, USA
Wischmeier et Smith (1978)	Logarithmic model	$KE = \alpha+\beta\log_{10}I$	North of America
Hudson (1961)	Linear model	$KE = a(I-b)$	Zimbabwe (Africa)

Table 2: Some erosivity factor (R) models developed in various studies:

Reference	Model R	Parameters	Location
Renard and Freimund (1994)	$R= a_1P^{b1}$ $R= a_2+b_2P^c$	a_1,b_1,a_2,b_2,c: nonlinear regression parameters	USA
Richardson et al. (1983)	$R_d = \alpha_1 P_d^{\beta 1}$	α_1, β_1: nonlinear regression parameters. P_d: daily rainfall	Morocco
Arnoldus (1977)	$R= a_3F^{b3}$ $F= \frac{\sum_{i=1}^{12} P_{i,max}^2}{P}$	a_3,b_3,a_2,b_2,c: linear regression parameters. $P_{i,max}$: monthly Rainfall ; P : yearly rainfall	Morocco
Roose E. (1977)	$R = \alpha+\beta P$	α, β: linear regression parameters. P : rainfall	West Africa Countries

These models (Tables 1 and 2) have been applied in several studies across many countries worldwide (Xie Y. et al., 2016; Vantas K. et al., 2018; Abadi M. et al., 2016; etc.) and particularly in Africa, notably in Nigeria (Igwe et al., 1999; Salako F., 2010) and South Africa (Smithern et al., 1982). However, most of these models were established based on rainfall data. In this study, the (KE) parameter is determined based on disdrometric data using the formula (2) demonstrated in a recent study conducted by ADJIKPE et al. (2021):

$$KE_j \, [J.m^{-2}h^{-1}] = \frac{3\pi}{10^4} \sum_{i=1}^{n} D_i^3 [V_t(D_i)]^3 \, N(D_i) \Delta D_i \tag{2}$$

where ($N(D_i)$) denotes the number of raindrops per unit volume and per diameter interval. It represents the analytical function commonly used to analyze the Drop Size Distribution (DSD) by several authors such as Sauvageot and Lacaux (1995), Ulbrich and Atlas (1998), Moumouni et al. (2008), Tenorio et al. (2012), etc. It is calculated as follows:

$$N(D_i) = \frac{N_i}{ST \Delta D_i V_t(D_i)} \tag{3}$$

D_i is the equivalent diameter of the measured raindrops. (ΔD_i) is the width of the diameter interval centered on (D_i). In this study, (D_i) and (ΔD_i) are expressed in millimeters. (S) is the collection surface area of the disdrometer expressed in square meters. At the end of the duration (T), (N_i) is the number of drops counted by the disdrometer in each diameter interval. ($V(D_i)$) is the fall velocity of drops with diameter (D_i). To ensure that the rainfall rate is proportional to a moment of the function (N(D)), the drop fall velocity proposed by Atlas and Ulbrich (1977) is used:

$$\mathrm{V_t(D_i) = 3.78 D_i^{0.67} [m \cdot s^{-1}]} \tag{4}$$

In all the aforementioned studies, $T = 1min = 60s$ and $N(D_i)$ expressed in $[m^{-3}mm^{-1}]$. The rainfall intensity (I) is the volume of water that falls per unit area and per unit time, and it is calculated in ADJIKPE et al. (2021) using the following formula:

$$I[mm.h^{-1}] = \frac{6\pi}{10^4} \sum_{k=1}^{n} D_i^3 V_t(D_i) \, N(D_i) \Delta D_i \tag{5}$$

The rainfall amount for each spectrum of an erosive rainfall event were calculated using formula (5). Since a significant portion of precipitation typically occurs within a small fraction of its duration, ranging from 5 minutes, 10 minutes, 15 minutes, 30 minutes to 60 minutes (Capolongo et al., 2008; Cattan et al., 2008; Fang et al., 2012), the maximum intensity over 30 minutes for each erosive rainfall event in the DATA Y sample is the maximum value of the rainfall intensities for all the DSD spectra of the erosive rainfall event. A model R_j-KE_j is established through linear regression of the erosivity factor (R_j), calculated using formula (1), on the total kinetic energy (KE_j), calculated using formula (2), for each erosive rainfall event (j). This model, in the form of a power law ($R_j = aKE_j^b$), where (a) and (b) are respectively the prefactor and the exponent, serves as an estimator for the erosivity factor (R_j) of an erosive rainfall event (j) based on its kinetic energy (KE_j). This parameter is also derived using the same method through a (KE_j-I_j) model. By combining the two models (R_j-KE_j) and (KE_j-I_j), another model (R_j-I_j) is obtained to estimate the erosivity factor (R_j) from the average intensity (I_j) of an erosive rainfall event (j).

2.4- Evaluation of the Performance of the (R_j-KE_j) and (R_j-I_j) Models

The evaluation of the performance of the models is conducted through the statistical criteria defined in **Table 3**. A model is considered effective if the correlation coefficient and the Nash efficiency criteria as well as the KGE (Kling-Gupta Efficiency) approach 1, while the relative bias approaches zero. All modeling is based on the DATA Y sample, and the ability of the constructed models to reproduce the erosivity factor of any erosive rainfall event is assessed using the erosive rainfall events from the DATA X sample.

Table 3: Statistical Criteria for Comparison

N°	Statistical Criteria	Expression
1	Pearson correlation coefficient	$\rho = \frac{E[(Y^{obs} - E[Y^{obs}])(Y^{est} - E[Y^{est}])]}{\sigma_{obs}\sigma_{est}}$
2	Nash efficiency criteria (Nash et Sutchiffe, 1970)	$Nash = 1 - \frac{E[(Y^{est} - Y^{obs})^2]}{E}$
3	Kling-Gupta efficiency criteria (Gupta et al., 2009)	$KG = 1 - \sqrt{(\rho - 1)^2 + (\frac{\sigma_{est}}{\sigma_{obs}} - 1)^2 + (\frac{E[Y^{est}]}{E[Y^{obs}] - 1})^2}$
3	relative bias	$Bias = \sum \left[\frac{(Y^{est} - Y^{obs})}{Y^{obs}}\right]$

3. Results and Discussion

3.1- Analysis of the Erosive Power of Precipitation

Figures 6, 7 and 8 illustrate the distribution of rainfall events by site, as well as their cumulative heights and total kinetic energies.

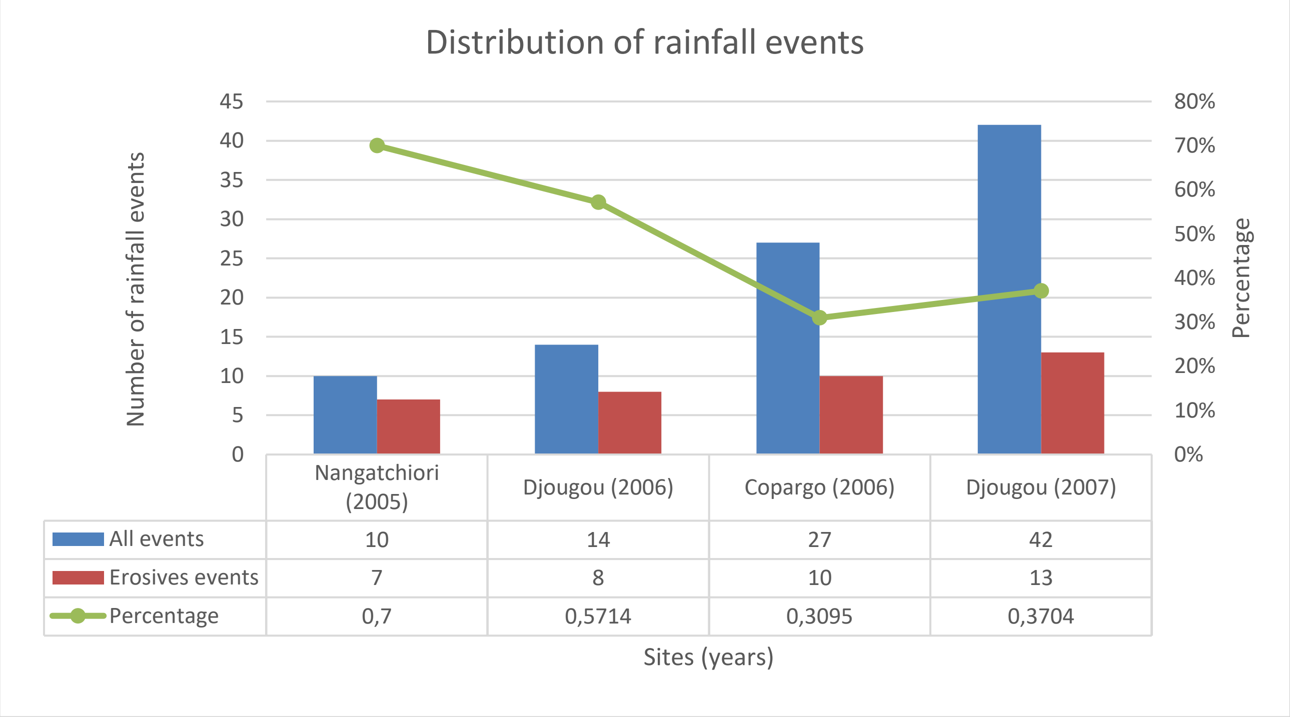

Figure 6: **Distribution of Rainfall Events by Sit**

This histogram shows that the highest percentage of erosive rainfall events (70%) occurred in 2005 at the Nangatchiori site, while the lowest (37%) was in 2007 at the Djougou site. Overall, the 38 identified erosive rainfall events represent 40.86% of the 93 measured events across the three sites in northern Benin.

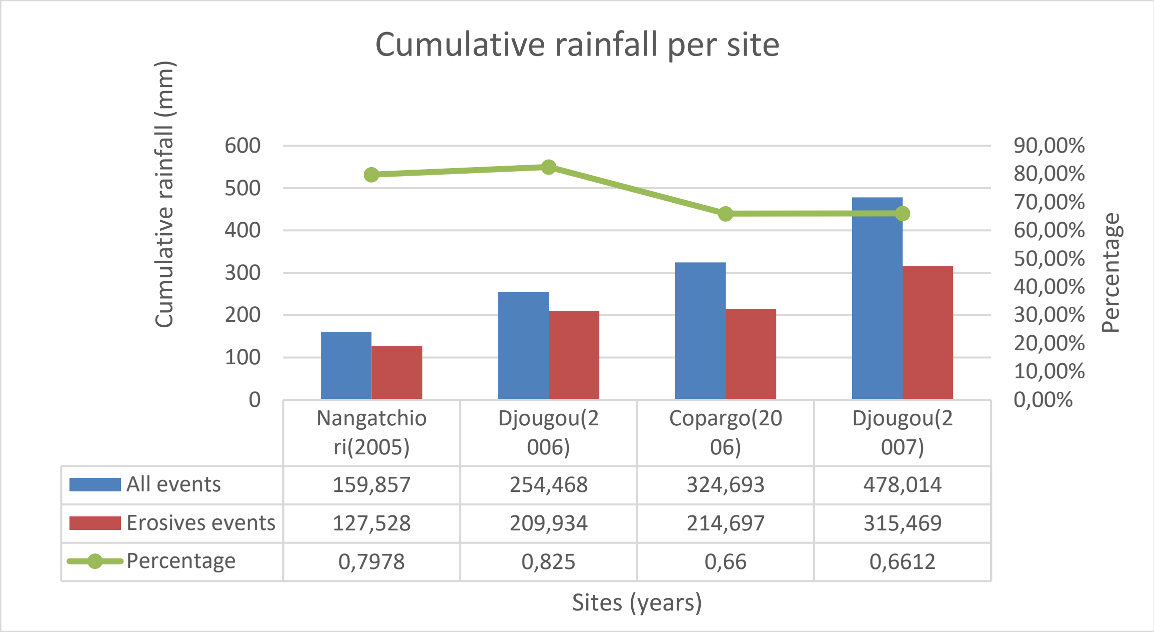

Figure 7: **Distribution of Cumulative Rainfall Heights by Site**

In 2006, the cumulative heights of erosive rainfall events at the Djougou site accounted for 82.50% of all events measured at that site, the highest percentage recorded. The lowest percentage (66%) of cumulative heights was in 2006 at Copargo. In total, 71.29% of the cumulative heights from all measured events from 2005 to 2007 came from the 40.86% of potentially erosive rainfall events.

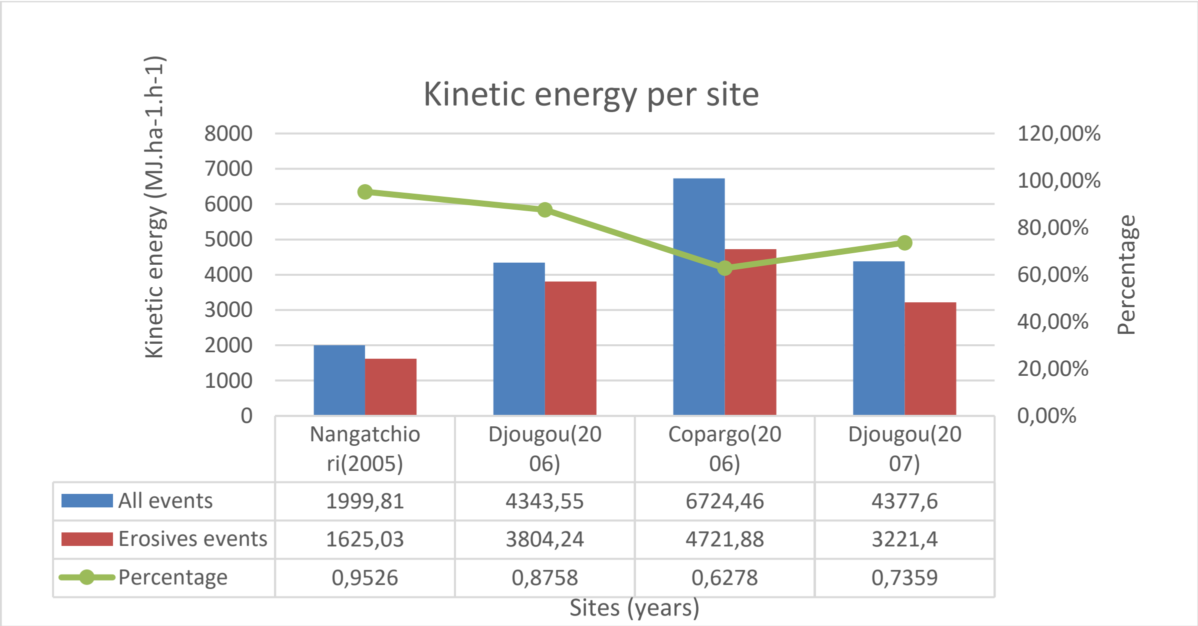

Figure 8: Distribution of Total Kinetic Energies of Rainfall Events by Site

The histograms in **Figure 8** show that the greatest percentage of total kinetic energy from erosive rain events is obtained at the Nangatchiori site in 2005 while the lowest percentage (63%) of total kinetic energy from erosive rain events was registered in 2006 on the Copargo website. Thus, erosive rain events which represent only 40.86% of all rain events sampled produced an overall percentage of 76.65% of total kinetic energy. The histograms in **Figures 6, 7 and 8** therefore allow us to deduce that 71.23% of the cumulative rainfall amounts and 76.65% of the total kinetic energy of all rain events comes from 40.86% of rain events identified as potentially erosive. In addition, the histograms in Figure 5 below present a comparison of the cumulative heights, maximum intensity and total kinetic energy of erosive rain events compared to all measured rain events.

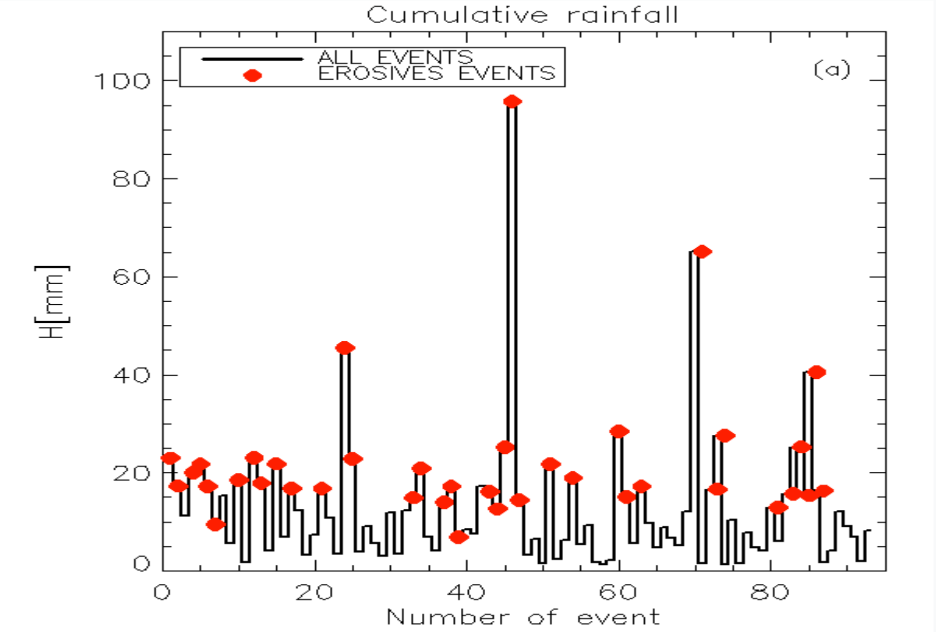

Figure n°9(a): Comparison of maximum intensities of rain events of erosive rain events to Those of all rain events

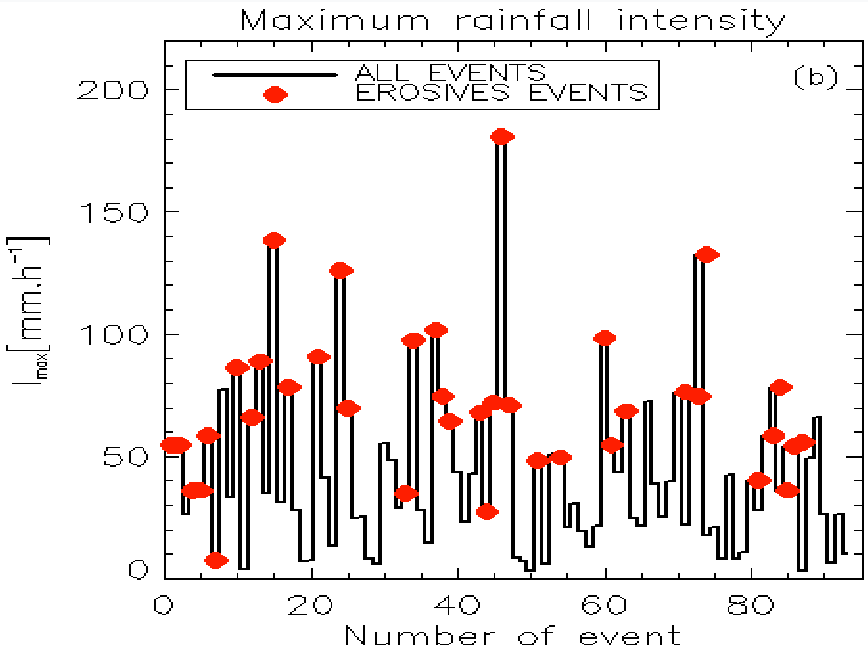

Figure n°9(b): Comparison of Total heights for each event of erosive rain events to those of all rain events

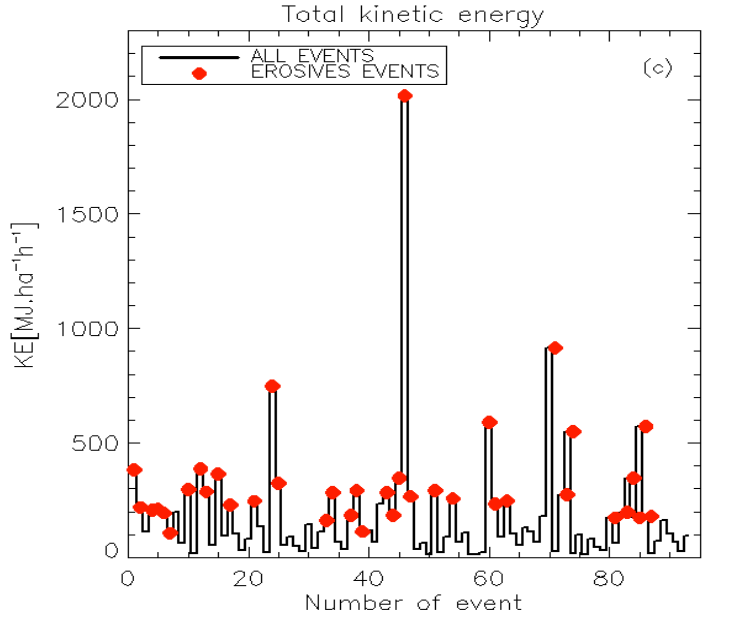

Figure n°9(c): Comparison of Total kinetic energies of each rain event of erosive rain events to those of all rain events.

On the histograms (a), (b) and (c) of **Figure 9**, we see that erosive rain events have the greatest accumulations of rain depth, maximum intensity and maximum kinetic energy. From the results of **Figures 6, 7, 8, 9**, it appears that erosive rainy events have great erosive power and are responsible for most of the erosive risks linked to Precipitation.

3.2 - Modeling the Erosivity Factor of Erosive Rainfall Events

Using the DATA X sample, the erosivity factor (R_j) of an erosive rainfall event (j) is calculated using Formula (1), while the total kinetic energy of the erosive rainfall events is determined using Formula (2). The model (R_j-KE_j), which establishes the relationship between the erosivity factor and total kinetic energy, is derived through a linear regression of (R_j) on the total kinetic energy (KE_j) for each erosive rainfall event (j). **Figure 10** shows the results of this regression.

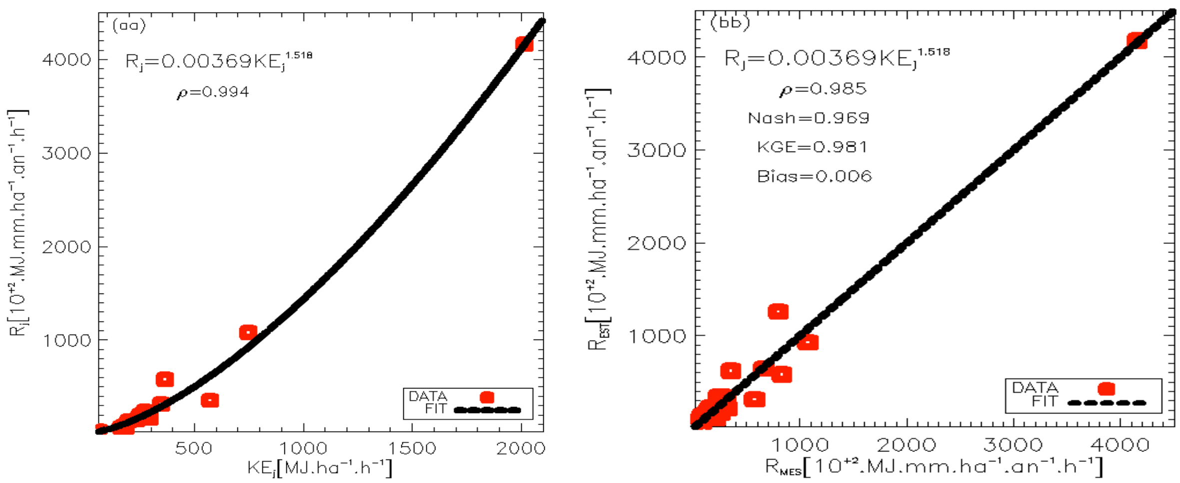

Figure n°10: Sample DATA Y: **graph (aa):** Adjustment of the erosive factor R_j on the total kinetic energy KE_j of erosive rain events; **graph (bb):** comparison of the erosivity factors measured and estimated using the DATA X sample; the black line represents the first bisector.

The R_j-KE_j model thus established between the erosive factor R_j and the total kinetic energy KEj of an erosive rainy event j is:

$$\mathbf{R_j = 0.00369KE_j^{1.518}} \quad \mathbf{(7)}$$

The Pearson correlation coefficient calculated between the erosivity factors measured and estimated by model (7) gives ρ = 99.4% (see graph (aa)). This coefficient tending towards 100% shows that the adjustment is of good quality. Likewise, we note a good distribution of the cloud of erosivity factors around the first bisector (**graph bb**) with Nash and KGE efficiency criteria calculated between the measured and estimated values of 96.9% and 98.1% respectively. These values also tend towards 1 and the relative bias is 0.6%. Which allows us to conclude that this model is effective in estimating the erosive factor of any erosive rainy event. The interest of this model lies in the fact that it makes it possible to directly estimate the erosive factor of an erosive rainy event from its total kinetic energy which is a quantity directly measurable today by certain sensors latest generation. When the kinetic energy is not available, it can be deduced from the rain intensity which is often available through a relationship between the kinetic energy KE_j and the rain intensity I_j of an erosive rain event j established by linear regression. **Figure 11** below shows the result of this regression.

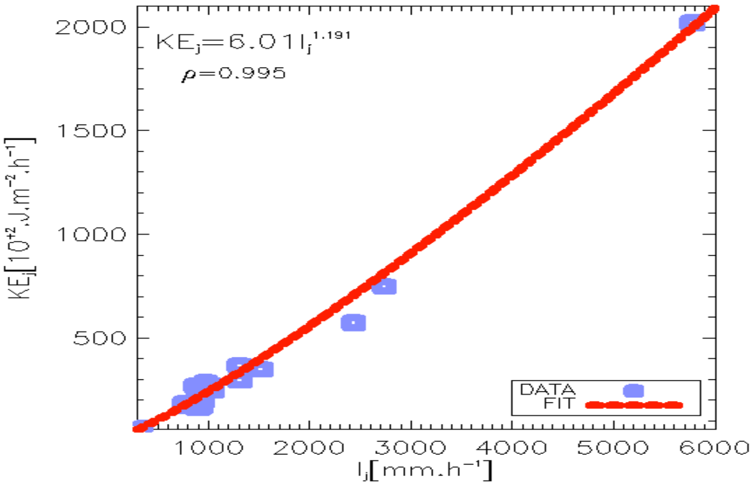

Figure 11: KE_j-I_j relationship established by linear regression of the erosivity factors R_j on the intensities Ij of the erosive rain events j of the DATA Y sample

The relationship thus obtained is:

$$KE_j = 6.01I_j^{1.191} \quad (8)$$

The relationship (8) thus established between the total kinetic energy KE_j and the average intensity I_j of an erosive rain event j is different from those obtained by ADJIKPE et al. (2021) on the same data. This difference is justified by the fact that these KE-I relationships were obtained at different integration time steps between the kinetic energy of a DSD spectrum and its intensity I. The capacity of relation (8) to reproduce the total kinetic energy of an erosive rain event is analyzed on the DATA X sample. Table no. 4 below shows the results of the statistical criteria calculated between the measured kinetic energies and estimated by the relation KE_j-I_j.

Table n°4: Performance of the KE_j - I_j relationship

Estimator	ρ	Nash	KGE	Bias
KE_j - I_j	0.9952	0.9796	0.9009	0.0495

Table n°4 shows that the values of the correlation coefficient and the Nash and KGE efficiency criteria calculated between the measured and estimated total kinetic energies (relation 8) tend towards 1 while the relative bias tends towards 0. Which proves that relation (8) can effectively estimate the total kinetic energy KE_j of any erosive rain event j. By introducing relation (8) into model (7) we obtain:

$$\mathbf{R_j = 0.0561 I_j^{1.808}} \qquad (9)$$

The adjustment of the erosivity factors Rj on the intensities Ij of the different erosive rainy events j is of very good quality as indicated on the graph in figure (8) with the values estimated by the Rj-Ij model very well correlated with the measured values (ρ=98.8%) as shown in **figure 12**.

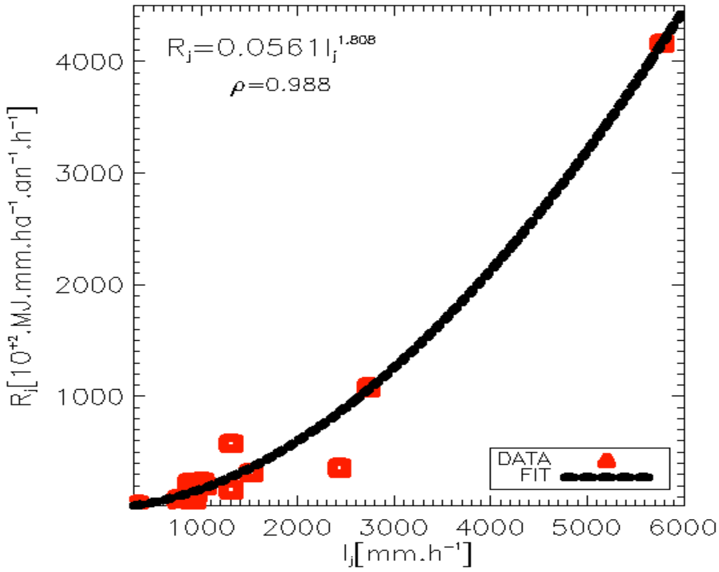

Figure 12: Model R_j-I_j established by linear regression of the erosivity factors R_j on the rain intensities Ij of the erosive rain events j of the DATA sample Y

3.3- Evaluation of the performance of the two models R_j-KE_j and R_j-I_j

To evaluate the ability of these models to estimate the erosivity factor of an erosive rain event, three criteria: the correlation coefficient, the Nash efficiency criterion and the relative bias are calculated between the measured and estimated erosivity factors. by the R_j-KE_j and R_j-I_j models. The graphs in **Figures 13** present the results obtained.

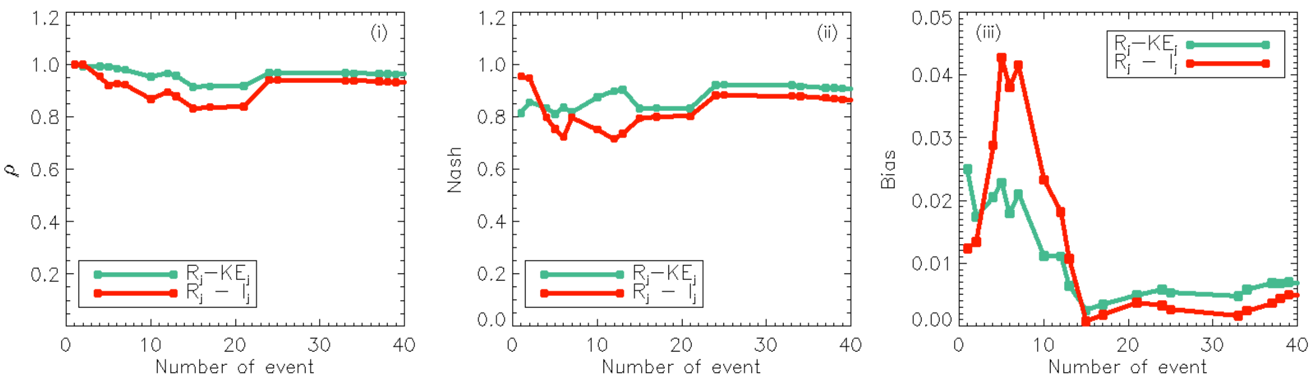

Figures 13: DATA X: Performance of models R_j-KE_j and R_j-I_j; (i) the correlation coefficient; (ii) the Nash efficiency criterion; (iii) the relative bias

The graphs in **figures 13** above show that the correlation coefficient and the Nash efficiency criterion calculated between the erosivity factors measured and estimated by the R_j-KE_j and R_j-I_j models tend towards 1; the lowest values of these two criteria are respectively greater than 80% and 70% while the relative bias on each measurement generally tends towards zero. The largest bias value is less than 5%. Furthermore, we note a downward trend in the Nash efficiency criteria and an upward trend in the relative bias when the erosive rain event has holes and this trend increases as the number of holes increases. between the spectra increase. These results, which highlight the influence of periods without rain on the criteria, show that the effectiveness of the model decreases depending on the duration without rain within the erosive rain event. To our knowledge, there are no bibliographic references on the R_j-KE_j and R_j-I_j models, allowing us to make a comparison. In any case, these two models are efficient and make it possible to estimate the erosive factor of any erosive rain event with good precision.

Conclusion

This work made it possible to understand that the erosive risk linked to precipitation is essentially due to potentially erosive rainy events. The latter, characterized by peaks of cumulative heights, maximum intensity and total kinetic energy, are then endowed with the greatest erosive powers which are reflected through the value of the rain erosivity factor or index. In this study, two models R_j-KE_j and R_j-I_j were established to estimate this quantity from data on the total kinetic energy (data provided today by numerous sophisticated sensors of the latest generation) or data on the rain intensity (data provided by most sensors). From the study of the efficiency and fidelity of these models, it appears that these models are efficient and can reproduce the erosivity factor of rain with good precision. This work also proved that the performance of these models decreases as the duration of the dry period within each erosive rain event increases.

ACKNOWLEDGEMENTS: Based on a French initiative, AMMA was built by an international scientific group and is currently funded by a large number of agencies, especially from France, UK,US,and Africa. It has been the beneficiary of a major financial contribution from the European Community's Sixth Framework Research Program. Detailed information on scientific coordination and funding is available on the AMMA International web site http://www.amma-international. org.

Competing Interests: The authors declare that this is original research conducted by the authors and is not under consideration for publication in any other journal or publication outlet. There is therefore no conflict of interest to declare.

CRediT Author Statement: ADJIKPE L.S.: Conceptualisation, , Supervision, Writing – Review and Editing. KOUGBEAGBEDE, O.E.: Conceptualisation, Supervision, Experimentation. GUEDJE K. F.: Experimentation, Writing – Original Draft, Writing – Review and Editing Ethical approval: Not required. Funding: No funding was received for this work. Disclosure: During the preparation of this manuscript, the authors used Quillbot® paraphrasing tool in order to improve the fluency and readability of some parts, with caution. The content was thereafter reviewed and edited as necessary and the authors take full responsibility for the content of the manuscript.

CONFLICT OF INTEREST The authors declare that they do not have any conflict of interest.

CRediT Author Statement: ADJIKPE L.S.: Conceptualization; methodology; modelling ; data curation ; Formal analysis ; Writing ; original draft; KOUGBEAGBEDE H. : Data curation; Formal analysis; Writing – original draft) ; F.K. GUEDJE K.F. : Supervision; critical and formal analysis ; MOUMOUNI S. : Supervision ; Formal and critical analysis ; MASSOU S. : Supervision ; critical analysis.

References.

Abadi M., Barham K., Chen J., Chen Z., Davis A., Dean J., Tensorflow: A system for large-scale machine learning. (2016). In: OSDI. pp. 265-283

Adjikpé L.S., Moumouni S., Kougbeagbede H. (2021). Potentiel érosif de la pluie : identification du meilleur estimateur d'énergie cinétique de la pluie à partir des données de drop size distribution (DSD) de pluies mesurées au nord-ouest du bénin. *Journal de physique de la SOAPHYS*, vol(2) http://www.soaphys.org/journal/ ISSN. Print : 2630-0958

Alsadi, J., Alkhatib, F., Antony, J., Garza-Reyes, J.A., Tortorella, G. and Cudney, E.A. (2024), "A systematic literature review with bibliometric analysis of Quality 4.0", *The TQM Journal*, Vol. ahead-of-print No. ahead-of-print. https://doi.org/10.1108/TQM-02-2024-0050

Arnoldus H.M.J. (1977). Methodology used to determine the maximum potential average 547 annual soil loss due to sheet and rill erosion in Morocco. *FAO Soils Bulletin*, 34: 39-51.

Atlas D. and C. W. Ulbrich (1977). Path and area-integrated rainfall measurement by microwave attenuation in the 1-3 cm band., *J. Appl. Meteor.*, 16, 1322-1331.

Brown L.C., Foster G.R. (1987). Storm erosivity using idealized intensity distributions. *Transaction of the American Society of Agricultural Engineers* 30, 379-386.

Capolongo D.a, Diodato N.B, Mannaerts C.M.C, Piccarreta M.A, Strobl R.O. (2008). Analyzing temporal changes in climate erosivity using a simplified rainfall erosivity model in Basilicata (southern Italy). *J. Hydrol*. 356 (1-2), 119–130.

Cattan P., Cabidoche Y., Lacas J., Voltz M. (2008). Effects of tillage and mulching on runoff under banana (Musa spp.) on a tropical Andosol. *Soil Till. Res*. 86 (1), 38–51. http://dx.doi.org/10.1016/j.still.2005.02.002

Cuéllar-Rojas O-A., Hincapié-Montoya M., Contero M. and Güemes-Castorena D. (2022) Bibliometric analysis and systematic literature review of the intelligent tutoring systems. *Front. Educ.* 7, 1047853. http://dx.doi.org/10.3389/feduc.2022.1047853

Delahaye J.Y., Barthès L., Golé P., Lavergnat J. and Vinson J.P. (2005). A dual-beam spectropluviometer concept, *J. Hydrology*, 328, 110-120.

Dunkerley D. (2008). Identifying individual rain events from pluviograph records: a review with analysis of data from an Australian dryland site. *Hydrol. Process*. 22, 5024–5036.

Dunkerley D. (2010). How do the rain rates of sub-event intervals such as the maximum 5- and 15-min rates (I_5 or I_{30}) relate to the properties of the enclosing rainfall event? *Hydrol. Process*. 24, 2425–2439.

Fang N.F., Shi Z.H., Li L., Guo Z.L., Liu Q.J., Ai L. (2012). The effects of rainfall regimes and land use changes on runoff and soil loss in a small mountainous watershed. *Catena* 99, 1–8. http://dx.doi.org/10.1016/j.catena.2012.07.004.

Grimm M., Jones R.J.A., Rusco E. and Montanarella, L. (2003). Soil erosion risk in Italy: a revised USLE approach. *EUR 20677 EN, Office for Official Publications of the European Communities, Luxemburg, Luxemburg, 26 p.*

Gupta H. V., H. Kling, K.K. Yilmaz and G.F. Martinez (2009). Decomposition of the mean squared error and NSE performance criteria: Implications for improving hydrological modelling: *J. Hydrol*., 377, 80-91, doi:10.1016/j.jhydrol.2009.08.003.

Hammouti B., Aichouch I., Kachbou Y., Azzaoui K., Touzani R. (2025) Bibliometric analysis of global research trends on UMI using Scopus database and VOS viewer from 1987–2024, *J. Mater. Environ. Sci.* 16 (4), 548-561

Hudson, N.W (1961). An introduction to the mechanics of soil erosion under conditions of subtropical rainfall. In Proceedings of the Proceedings of the Rhodesian Scientists Association 49; Oxford University Press: Oxford, UK, 1961; pp. 15–25.

Huff (1967). Time distribution of rainfall in heavy storms. *Water Resour. Res.* 3 (4), 1007–1019.

Jan Pétrù and Jana KALIBOVÁ (2018). Measurement and Computation of Kinetic Energy of Simulated Rainfall in Comparison with Natural Rainfall. *Original Paper Soil & Water Res.*,13(4), 226–233. https://doi.org/10.17221/218/2016-SW

Igwe C, Mbagwu J, Akamigbo F (1999). Application of SLEMSA and USLE models for potential erosion hazard mapping in south-eastern Nigeria. *International Agrophysics.*13, 41-48

Kougbéagbédé H., B. E. Houngninou and S. Moumouni (2017). Modeling Rain Rate Distribution Per Diameter Class from Disdrometer Data Collected in Northern Benin (AMMA Campaign): A New Relationship Between Radar Reflectivity and Rainfall Rate: *International Journal of Research and Innovations in Earth Science*, 4 (3), ISSN (Online): 2394-1375.

Löffler-Mang M., and J. Joss. (2000). An Optical Disdrometer for Measuring Size and Velocity of Hydrometeors. *J. Atmos. Oceanic. Technol.*, 17, 130-139.

Lrhoul H., Turki H., Hammouti B. (2023), Benammar O., Internationalization of the Moroccan Journal of Chemistry: A bibliometric study, *Heliyon*, 9(5), e15857, ISSN 2405-8440, https://doi.org/10.1016/j.heliyon.2023.e15857

McGregor, K.C.; Bingner, R.L.; Bowie, A.J.; Foster, G.R. (1995). Erosivity index values for Northern Mississippi. *Trans. ASAE*, 38, 1039–1047.

Mehta N., Kozielska B. (2024), A systematic literature review and bibliometric analysis of sources and analytical approaches of indoor microplastics, *Emerging Contaminants*, 10, Issue 1, 100274, ISSN 2405-6650, https://doi.org/10.1016/j.emcon.2023.100274

Mishra, A.K., Singh, V.P. (2010), A review of drought concepts, *Journal of Hydrology*, 391(1-2), 202–216

Moumouni S., F.P. Akponi, E.P. Zahiri (2023). Impact of integration time steps of rain drop size distribution on their double-moment normalization: a case study in northern Benin. *Comptes Rendus Geoscience-Sciences de la Planete*, 355, 109-133. https://doi.org/10.5802/crgeos.200

Moumouni S., Adjikpé L. S., and Lawin A. E. (2021). Impact of integration time steps of rain drop size distribution on their structuring and their modelling: A case study in Northern Benin, *C. R. Geosci.*, 353(1), 135–153.

Moumouni S., Adjikpé L. S., Massou S., and Lawin A. E. (2018). Parameterization of drop size distribution with rainfall rate: comparison of the N(*D*) and R(*D*) functions; and relationship between gamma and lognormal laws. *Int. J. Res. Innov. Earth Sci.*, 5(6), 116–123.

Moumouni S., Gosset M., Houngninou E. (2008). Main features of rain drop size distributions observed in Benin, West Africa, with optical disdrometres. *Geophys. Res. Lett.*, 35, article no. L23807.

Nan Yu B. Boudevillain and G. Delrieu. (2012). Estimation of rain kinetic energy from radar reflectivity and/or rain rate based on a scaling formulation of the raindrop size distribution. *Water Resources Research*, 48, w04505, doi:10.1029/2011wr011437.

Nash J. E. and J. V. Sutcliffe (1970). River flow forecasting through conceptual models part I - A discussion of principles. *J. Hydrol.*, 10, 282-290.

N'diaye A.D., Kankou M.S.A., *et al*. (2022). A review of biomaterial as an adsorbent: From the bibliometric literature review, the definition of dyes and adsorbent, the adsorption phenomena and isotherm models, factors affecting the adsorption process, to the use of typha species waste as adsorbent. *Communications in Science and Technology*, 7(2), 140-153. https://doi.org/10.21924/cst.7.2.2022.977

Petkovsek G. and Mikos, M. (2004). Estimating the R-factor from daily rainfall data in the sub-Mediterranean climate of southwest Slovenia. *Hydrological sciences journal*, 49: 869-877.

Renard K. G. et Freimund J. R. (1994). Using monthly precipitation data to estimate the R factor in the revised USLE. *J. Hydrol*. 157, 287–306.

Richardson C.W., Foster G.R., and Wright, D.A. (1983). Estimation of erosion index from daily rainfall amount. *Trans. Am. Soc. Agric. Eng*. 26: 153–1

Roose, E. (1994). Introduction à la gestion conservatoire de l'eau, de la biomasse et de la fertilité des sols. *Bulletin Pédologique* FAO, n° 70, 420 p.

Salako F (2010). Development of isoerodent maps for Nigeria from daily rainfall amount. *Geoderma*, 156(3), 372-378

Salim R., E.H. Loukili, Ech-chihbi E., Merimi C. (2022). Insight on the scientific production of USMBA until 2022: bibliometric analyses, *J. Appl. Sci. Envir. Stud* 5 (4), 219-230

Salles, C., J. D. Creutin, and D. Sempere-Torres (1998), The optical spectropluviometer revisited, *J. Atmos. Oceanic Technol.*, 15, 1215 – 1222.

Sauvageot H., Lacaux J. P. (1995). The shape of averaged drop size distributions. *J. Atmos. Sci., vol.* 52, 1070-1083.

Smithen A, Schulze R (1982). The spatial distribution in Southern Africa of rainfall erosivity for use in the universal soil loss equation . *Water SA.*, 8(2), 74-78

Tenorio R. S., da Silva Moraes M. C., Sauvageot H. (2012). Raindrop size distribution and radar parameters in Coastal Tropical Rain Systems of Northeastern Brazil," *J. Appl. Meteor. Clim.*, 51, 196-1970.

Ulbrich C. W. and D. Atlas (1998). Rainfall microphysics and radar properties: Analysis methods for drop size spectra. *J. Appl. Meteor.*, 37, 912-923.

Vantas K. Hydroscoper (2018): R interface to the Greek National Data Bank for hydrological and meteorological information. *Journal of Open Source Software*, 3(23), 625

Wischmeier, W.H. et D.D. Smith. (1978). Predicting rainfall erosion losses : A guide to conservation planning. *Agricultural handbook* N° *537, US department of Agriculture Science and Education Administration*, Washington, DC, USA, 163 p.

Xie Y., Yin S., Liu B., Nearing MA, Zhao Y. (2016). Models for estimating daily rainfall erosivity in China. *Journal of Hydrology*. 535, 547-558

(2025) ; http://www.jmaterenvironsci.com